Available online at www.sciencedirect.com
ScienceDirect
Ceramics International 36 (2010) 2441–2447
CERAMICS INTERNATIONAL
www.elsevier.com/locate/ceramint

Synthesis of organized hydroxyapatite (HA) using triton X-100

Jingxian Zhang *, Dongliang Jiang, Junling Zhang, Qingling Lin, Zhengren Huang

The State Key Lab of High Performance Ceramics and Superfine Microstructure, Shanghai Institute of Ceramics, Chinese Academy of Sciences, 1295 Dingxi Road, Shanghai 200050, China

Received 7 April 2010; received in revised form 16 April 2010; accepted 2 July 2010
Available online 7 August 2010

Abstract

In this article, highly organized HA nanostructure was developed using a nonionic surfactant *p*-(1,1,3,3-tetramethylbutyl) phenoxypoly (oxyethylene) glycol (triton X-100) as the template. The obtained well-organized architectural units were examined using transmission electron microscopy (TEM), SEM, XRD and FTIR. High-resolution transmission electron (HRTEM) revealed that HA nanorods were well assembled in order along the *c*-axis. FTIR results indicated the possible interactions between triton X-100 and HA. The mechanism of the assembly of well-oriented nanostructure was proposed. The composites containing nanosized hydroxyapatite with structural features close to that of human bone should be useful and important for the practical applications, especially in the development of biomimetic materials.

Keywords: Biomaterials; Precipitation; Nanostructures; Nucleation

1. Introduction

Hydroxyapatite (HA), a major inorganic component of bone, has been used extensively for biomedical implant applications and bone regeneration due to its bioactive and osteoconductive etc. properties [1–3]. However, the application of pure HA is very limited due to its brittleness.

Human bone is an inorganic–organic material consisting mainly of collagen fibres and nanosized, needle-like hydroxyapatite crystals. Collagen molecules exert a remarkable level of control over the nucleation, the size and the orientation of hydroxyapatite crystals and over the assembly of nanocrystallites as building blocks into hierarchy complex structures to achieve the extraordinary durability and strength [4,5]. It was presumed that the acidic extracellular matrix proteins that are attached to the collagen scaffold play important templating and inhibitory roles [6–9]. This ability to direct the assembly of nanoscale components into controlled and sophisticated structures has motivated intense efforts to develop assembly methods that mimic or exploit the recognition capabilities and interactions found in biological systems [10,11].

To duplicate this high performance of natural bone, artificial bone materials have been produced in which organic substrates such as poly(lactic acid), poly(L-lactide), peptide-amphiphile nanofibers, reconstituted collagen, and inorganic substrate have been used in the mineralization [12–21]. However, results are far from satisfying due to the difficulty in manipulating the position and orientation of HA nanoparticles.

Surfactants with hydrophilic and hydrophobic groups are often employed to direct organized superstructures due to their specific self-assembly behavior in solutions [22]. In the work of Clarkson and coworkers [23], the surfactant-docusate sodium salt was utilized to modify HA nanorods with a hydrophobic surface, and then these hydrophobic HA nanorods were organized into an enamel prism-like structure induced by solvent evaporation. Stupp and Braun designed self-assembling, synthetic substitutes for collagen, which can act as templates for hydroxyapatite crystallization [24]. Chen et al. used dodecylamine as the template and ordered hydroxyapatite (HA) nanorods were prepared after a hydrothermal treatment [25]. Recently, Ye et al. prepared oriented HA using P123 and tween 60 as the template [26].

Herein, biocompatible and biodegradable nonionic surfactants triton X-100 was utilized to biomimetically synthesize the oriented organization of HA nanorods. The synthesized samples were characterized by scanning electron microscopy

* Corresponding author.
E-mail address: jxzhang@mail.sic.ac.cn (J. Zhang).

0272-8842/$36.00
doi:10.1016/j.ceramint.2010.08.002

(SEM), X-ray diffraction (XRD), Fourier transform infrared spectroscopy (FTIR), nitrogen sorption, transmission electron microscopy (TEM) and high-resolution TEM (HRTEM).

2. Experimental procedures

2.1. Preparation of triton X-100/hydroxyapatite composites

Triton X-100 (*p*-(1,1,3,3-tetramethylbutyl) phenoxypoly(oxyethylene) glycol) (composition $C_{14}H_{22}O(C_2H_4O)_n$ (n = 9–10) was used as the structure directing agent. Triton X-100 is a nonionic surfactant which has a hydrophilic polyethylene oxide group (on average it has 9.5 ethylene oxide units) and a hydrocarbon lipophilic or hydrophobic group. It is related to the Pluronic range of detergents marketed by BASF Corporation. $Ca(NO_3)_2{\cdot}4H_2O$ (Sinopharm Chemical Reagent Co. Ltd) and $(NH_4)_2HPO_4$ (Sinopharm Chemical Reagent Co. Ltd) were of analytic grade and used without further purification.

Triton X-100 aqueous solution was prepared by dropping the suitable amount of triton X-100 into distilled water. After conditioning, the solution was added into a 0.02 M $(NH_4)_2HPO_4$ solution and the solution pH was adjusted to 11 using NaOH. Then 0.0334 M $Ca(NO_3)_2{\cdot}4H_2O$ solutions were gradually added to the triton X-100/$(NH_4)_2HPO_4$ solutions(the solution pH was pre-adjusted to 11 with NaOH) under stirring. The HA/X-100 mass ratio was calculated assuming that all the $Ca(NO_3)_2{\cdot}4H_2O$ was transformed into HA after reaction. The temperature of the solutions was varied from room temperature to 80 °C using water bath. After finishing, the mixture was aged at room temperature for 24 h before filtration. The powder was freeze-dried subsequently.

2.2. Characterization of triton X-100/hydroxyapatite composites

Powder XRD patterns were obtained on a Rigaku D/MAX-2550V diffractometer at 40 kV and 25 mA. Scans were run from 10° to 70° (2θ) at a speed of 4°/min and a step of 0.02° using Cu Ka X-rays (wavelength of 1.5418 Å). TEM analysis was performed using a JEOL 2100F electron microscope with an accelerating voltage of 200 kV. Interaction between triton X-100 and nano-HA powder was determined using a Fourier transform infrared spectrometer in the 400–4000 cm^{-1} region using a KBr wafer technique, scans were run from 4000 to 400 cm^{-1}, with data spacing 3.857 cm^{-1}. Microstructures of the samples were observed by field emission scanning electron microscopy (FESEM, JSM-6700F, JEOL, Tokyo, Japan).

3. Results and discussion

The XRD diffraction pattern of HA-triton X-100 composite (triton X-100/HA mass ratio is 0.2) and the pure HA grains were shown in Fig. 1. Similar to that observed using sodium salt carboxymethyl cellulose (CMC) as the template [27], the development of HA-triton X-100 composite directly depends on the triton X-100/HA mass ratio. The HA crystals that were

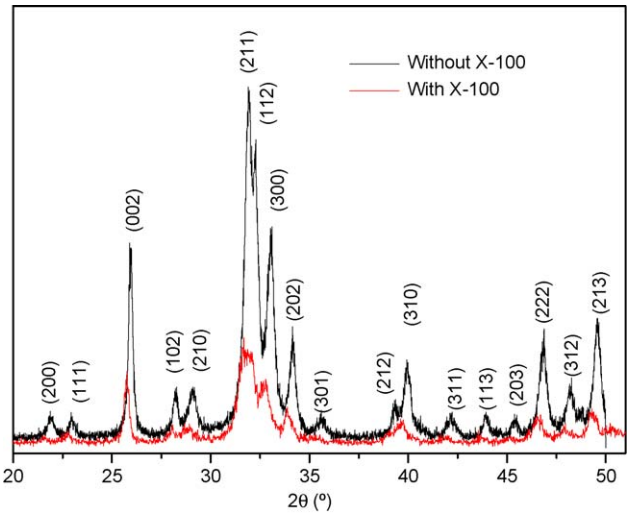

Fig. 1. XRD pattern of pure HA and HA-triton X-100 composites (pure HA phase).

synthesized without triton X-100 revealed the characteristic peaks of HA in the XRD pattern that were consistent with JCPDS files (9-432). Due to the ultrafine nature of the powder, peak broadening was observed in the X-ray diffraction pattern. After the addition of triton X-100, all the diffraction peaks corresponded to the standard characteristic peaks of hexagonal HA (JCPDS (Joint Committee for Powder Diffraction Standards) No. 09-0432), indicating the phase of the samples was consistent with that of highly pure HA. In the presence of triton X-100, a decrease in the peak intensity was observed. However, the preferred orientation of plane (0 0 2) was maintained in the sample series.

The crystallite size was calculated by Scherrer's equation. The crystallinity (Xc), corresponding to the fraction of crystalline apatite phase, was deduced according to Ref. [28]. For each point, three samples were prepared and tested with the average presented. The size of synthetic crystals varies with temperature and X-100 content, Fig. 2. The temperature shows a significant influence on the grain size and crystallinity, this is in well agreement with the result shown in the literature [29], Fig. 2a. It was shown that the triton X-100 content had a slight influence on the grain size and crystallinity degree (χ_c) of HA: For instance, the synthetic crystals with no X-100 was bigger than those with X-100, and the higher the X-100 content, the smaller the particle size and the lower the crystallinity degree, Fig. 2b, this might suggest the possible interaction between X-100 and HA.

Fig. 3 shows the TEM analytical results of the prepared synthetic crystals at different temperature with the X-100/HA mass ratio as 0.2. At room temperature, the synthesized HA grains were not well aligned. The increase of temperature to 60 °C led to a well alignment of HA grains. Further increase the temperature did not show any improvement in alignment. This might be due to the fact that with the increase in temperature, the hydrophilic PEO segment in X-100 will become more hydrophobic and could not self-assembly into well-ordered structure. Based on these results, the temperature was kept at 60 °C for the following study.

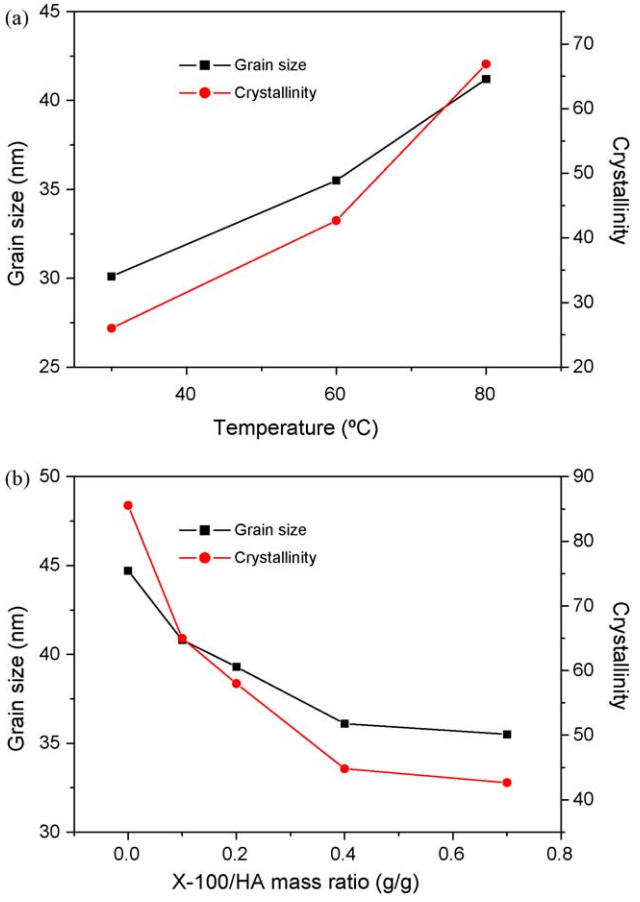

Fig. 2. Influence of the temperature (a) and X-100 content (b) on the size and crystallinity of HA grains (for each point, three samples were prepared and tested with the average presented).

Fig. 4 shows the TEM images of the assemblies of HA with different X-100 content. It was shown that in the presence of triton X-100, HA nanorods tend to be aligned and formed big particles. In Fig. 4b–e, these assemblies appeared to be comprised of bundles of the same size nano-HA rods aligned parallel to each other to yield an ordered matrix of island. However, with the increase of triton X-100/HA ratio up to 0.4, a less ordered structure was evidenced. At higher triton X-100/HA mass ratio of 0.7, a less ordered structure was developed too and mesopores appeared. In order to obtain well-organized HA structure, the triton X-100/HA mass ratio was kept between 0.1 and 0.2 in the subsequent experiment.

The HRTEM images (Fig. 5a) and selected area electron diffraction (SAED) pattern (Fig. 5b) indicate that all these synthetic nanorods were single crystals with a typical apatite crystalline structure. The crystal lattice planes were perfectly aligned and the lattice spacing was 0.346 nm, corresponding to the interplanar spacing of (0 0 2) planes for hexagonal HA. This reveals that the growth of HA occurs in the [0 0 2] direction and suggests that the building blocks of oriented attachment of HA nanorods are self-organized into ordered structures similar to that of human bones.

Fig. 6 demonstrates the SEM micrographs of samples. Bundles of nanorod-like HA crystals were observed in sample,

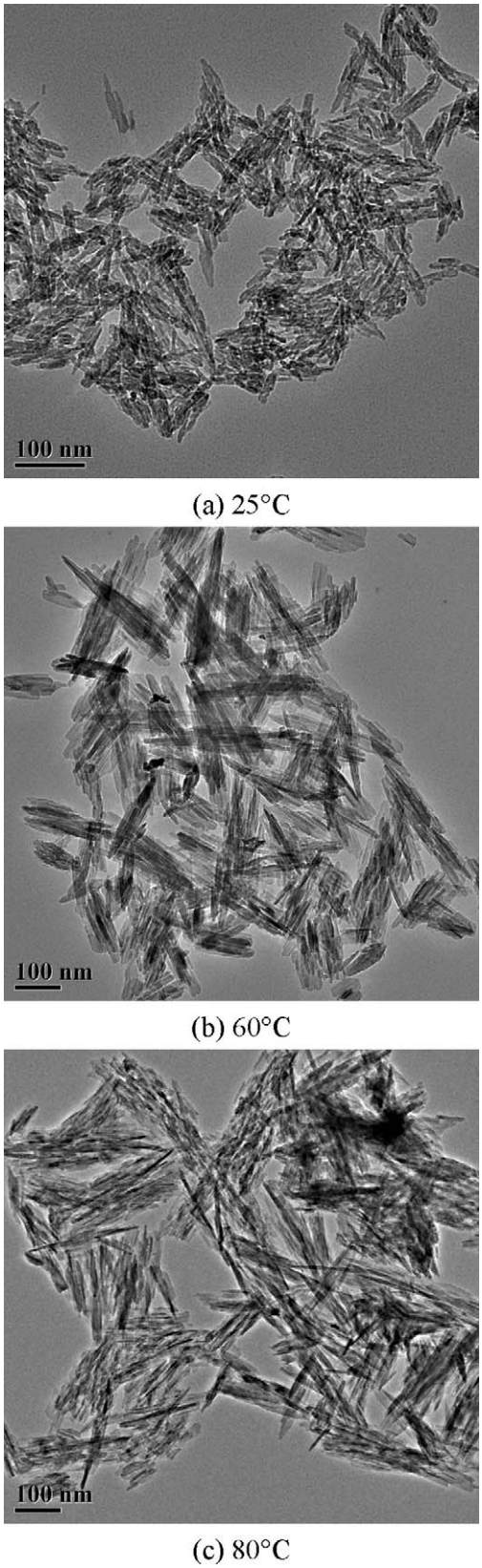

Fig. 3. Micrographs of HA composites synthesized at different temperature (X-100/HA mass ratio is 0.2).

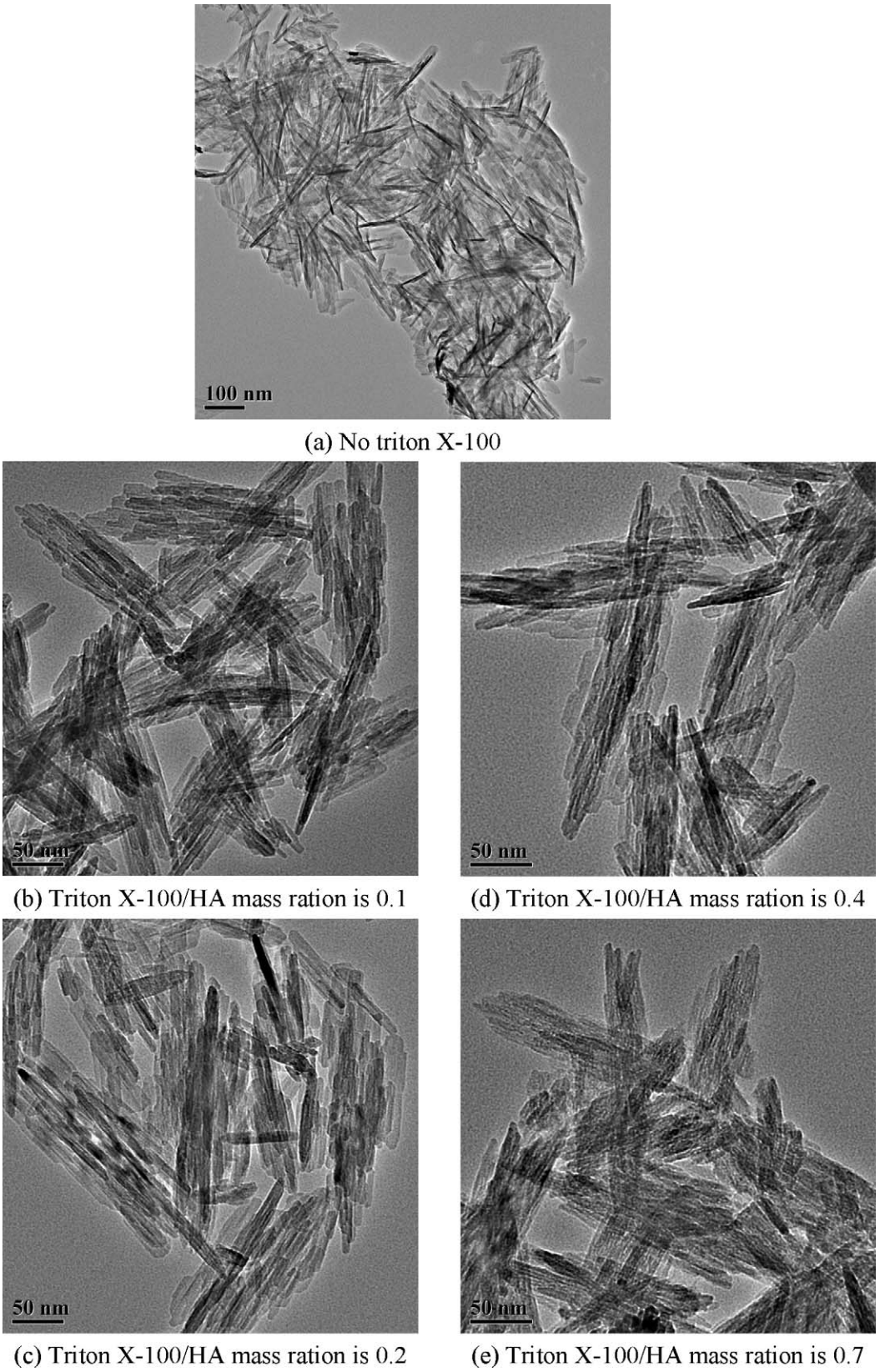

Fig. 4. The influence of triton X-100 content on the alignment of HA grains prepared at 60 °C.

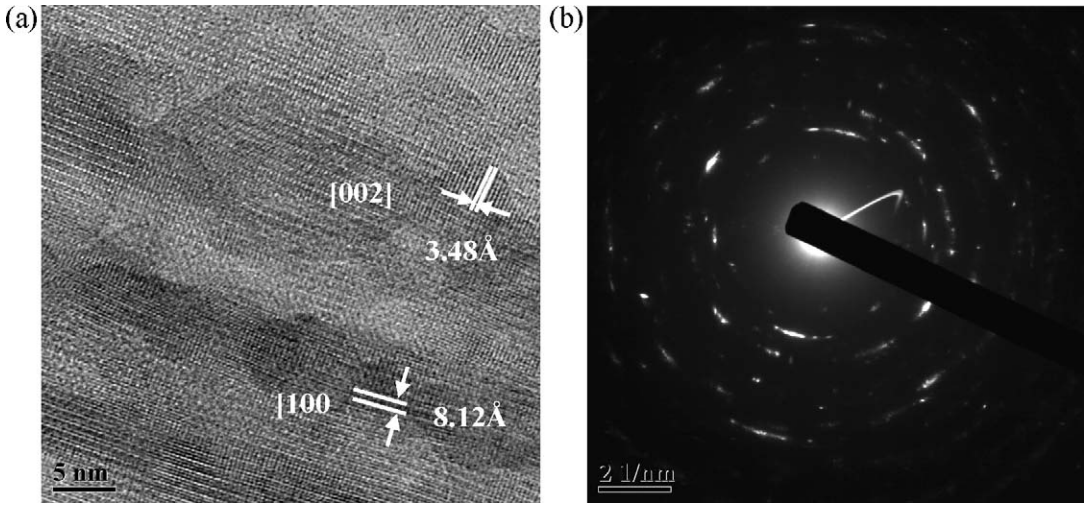

Fig. 5. HRTEM and election diffraction pattern of HA composites prepared at 60 °C (triton X-100/HA mass ration is 0.2).

in agreement with the TEM observation. Based on the above study, the suitable temperature and the X-100/HA mass ratio were selected as 60 °C and 0.1–0.2, respectively. The EDS data show that the Ca/P ratio of these synthetic crystals is 1.65, which is similar to the reported Ca/P molar ratio of HAp prepared in labs [30].

An FTIR spectrum shown in Fig. 7 was carried out in order to study the composition of the samples. The FTIR spectra showed that the P–O bond of the phosphate group's stretching and bending vibration remained in the same position at 1097, 1032, 962, 604, and 564 cm^{-1}. This indicates that all these prepared nanorods retained the same apatite crystalline structure in the experimental range. The weak bands at 871, 1400 and 1483 cm^{-1} were ascribed to CO_3^{2-} band positions, indicating that these groups may have incorporated into the HA crystal structure and replaced PO_4^{3-} groups [31]. (The 1483 cm^{-1} band is the overlap of the both peaks of $–CH_2$ and $–CO_3^{2-}$.) The carbonate might come from the atmosphere carbon dioxide during dissolving, stirring and reaction processes. The bands at 2922, 2854, 2972 cm^{-1} were ascribed to $–CH_2$ groups, indicating the existence of surfactant chains within the HA particles. Compared with pure HA, samples had

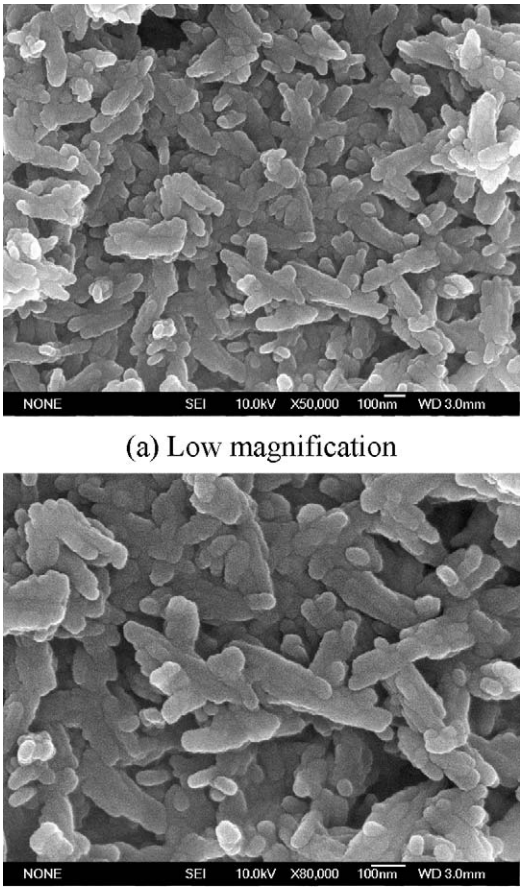

Fig. 6. Micrograph of HA composites prepared at 60 °C (triton X-100/HA mass ratio is 0.2).

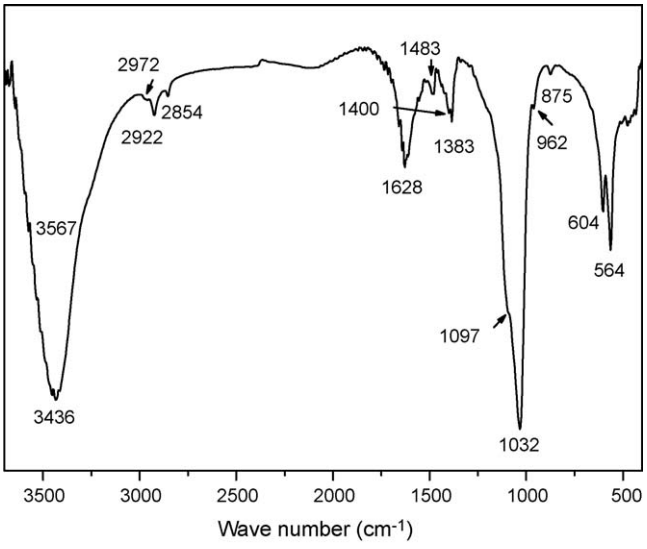

Fig. 7. FTIR spectra of HA composites.

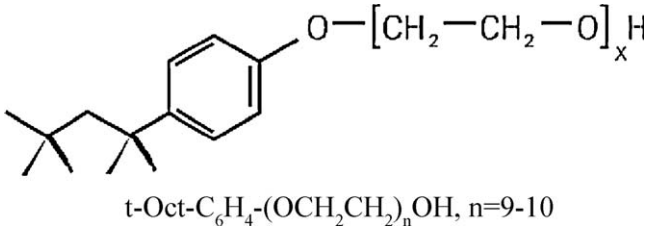

Fig. 8. Triton X-100 structures.

a weak stretching vibration mode of the OH groups at 3570 cm^{-1} and no librational vibration mode at 633 cm^{-1} was observed [32], implying the possible interaction between the surface groups of HA and the EO groups of X-100. This is similar to the case using P123 and tween 60 as the template [26]. It was reasonable to deduce that the hydrophilic end of X-100 have similar binding ability to hydroxyapatite rods as that of P123 and tween 60 and would therefore bind to hydroxyapatite nanorods.

The structure of triton X-100 is shown in Fig. 8. This formation of well-aligned HA nanoparticles is presumably templated by triton X-100, similar to the case in the natural bone that guided by collagen. Initially, in aqueous solution, triton X-100 tends to form the hexagonal phase after micellar solution [33], Fig. 9. Robson and Dennls proposed that the center of the core of triton X-100 micellar was hydrophobic consisting of octylphenyl groups and the shell was hydrophilic with oxyethylene groups extending outward through the core [34]. It was possible that the EO segments in X-100 coordinate with Ca^{2+} ions, similar to that observed between monosaccharide and Ca^{2+} ions [35,36]. After the addition of phosphorous source, the Ca^{2+} ions and PO_4^{3-} might co-precipitate on the hydrophilic surface of X-100 micelle and formed the precursor of HA. With the proceeding of the precipitation process, the precursor cluster with critical size was formed by adsorbing more phosphates and Ca^{2+} ions. In this way, the micelles acted as interactive templates where the organic/inorganic superstructure was developed in which nanoscaled calcium phosphate entities were interspersed with ordered domains. This formation of complexations between HA grains and triton X-100 molecule might lead to the alignment of small HA crystallites along the triton X-100 molecule, Fig. 9. Though the interactions was quite mild, the HA nano-grains was found to be well assembled. Further study on the templating mechanism is in process. This triton X-100/HA composite with well-controlled grain size and orientation of HAp nanorods might extend the understanding of biomineralization process and is also useful for the development of biomimetic materials.

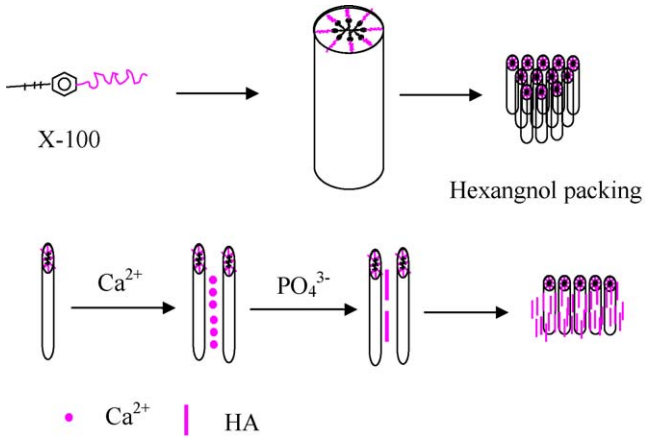

Fig. 9. Scheme of the formation process of the well-aligned HA nanorods.

4. Conclusions

Novel HA composites with various triton X-100/HA mass ratios were prepared using the co-precipitation method. In the composites obtained, calcium phosphate formed crystalline HA nanorods and a self-assembly phenomenon of HA nanocrystals along c-axes can be observed. Triton X-100 molecules were found to be effective to control the particle size of HA and the subsequent alignment of them. This might be due to the EO segments in triton X-100 which can attract Ca^{2+} ions and thus guide the growth of HA grains. The self-assembled organized structures of hydroxyapatite nanorods were similar to the hierarchy structure of human bones. This work shows the potential of applying nanotechnology to the direct bottom-up creation of scaffolds for bone tissue engineering applications.

Acknowledgements

This work was supported by the National Natural Science Foundation of China (No. 50772128), Shanghai Science and Technology Committee (Nos. 07DJ14001, 07pj14094), and the State Key Laboratory of High Performance Ceramics and Superfine Microstructures.

References

[1] L.L. Hench, Bioceramics, J. Am. Ceram. Soc. 81 (1998) 1705–1728.
[2] R.H. Doremus, Bioceramics, J. Mater. Sci. 27 (2) (1992) 285–297.
[3] J.M. Gomez-Vega, E. Saiz, A.P. Tomsia, G.W. Marshall, S.J. Marshall, Bioactive glass coatings with hydroxyapatite and Bioglass® particles on Ti-based implants: 1. Processing, Biomaterials 21 (2) (2000) 105–111.
[4] S. Weiner, H.D. Wagner, The material bone: structure–mechanical function relations, Annu. Rev. Mater. Sci. 28 (1998) 271–298.
[5] A.M. Belcher, X.H. Wu, R.J. Christensen, P.K. Hansma, G.D. Stucky, E. Morse, Control of crystal phase switching and orientation by soluble mollusc-shell proteins, Nature 381 (1996) 56–58.
[6] P.A. Raj, M. Johnsson, J.M. Levine, G.H. Nancollas, Salivary statherin. Dependence on sequence, charge, hydrogen bonding potency, and helical conformation for adsorption to hydroxyapatite and inhibition of mineralization, J. Biol. Chem. 267 (1992) 5968–5976.
[7] R.H. Clark, A.A. Campbell, L.A. Klumb, C.J. Long, P.S. Stayton, Protein electrostatic surface distribution can determine whether calcium oxalate crystal growth is promoted or inhibited, Calcif. Tissue Int. 64 (1999) 516–521.
[8] L. Addadi, S. Weiner, Interactions between acidic proteins and crystals—stereochemical requirements in biomineralization, Proc. Natl. Acad. Sci. 82 (1985) 4110–4114.
[9] A. George, L. Bannon, B. Sabsay, J.W. Dillon, J. Malone, A. Veis, N.A. Jenkins, D.J. Gillbert, N.G. Copeland, The carboxyl-terminal domain of phosphophoryn contains unique extended triplet amino acid repeat sequences forming ordered carboxyl-phosphate interaction ridges that

may be essential in the biomineralization process, J. Biol. Chem. 27151 (1996) 32869–32873.
[10] A.P. Alivisatos, K.P. Johnsson, X.G. Peng, T.E. Wilson, C.J. Loweth, M.P. Bruchez Jr., P.G. Schultz, Organization of 'nanocrystal molecules' using DNA, Nature 382 (6592) (1996) 609–611.
[11] C.A. Mirkin, R.L. Letsinger, R.C. Mucic, J.J. Storhoff, A DNA-based method for rationally assembling nanoparticles into macroscopic materials, Nature 382 (6592) (1996) 607–609.
[12] J.-H. Bradt, M. Mertig, A. Teresiak, W. Pompe, Biomimetic mineralization of collagen by combined fibril assembly and calcium phosphate formation, Chem. Mater. 11 (10) (1999) 2694–2701.
[13] F. Miyaji, H.-M. Kim, S. Handa, T. Kokubo, T. Nakamura, Bonelike apatite coating on organic polymers: novel nucleation process using sodium silicate solution, Biomaterials 20 (10) (1999) 913–919.
[14] N. Ignjatović, S. Tomić, M. Dakić, M. Miljković, M. Plavšić, D. Uskoković, Synthesis and properties of hydroxyapatite/poly-L-lactide composite biomaterials, Biomaterials 20 (9) (1999) 809–816.
[15] A. Bigi, E. Boanini, S. Panzavolta, N. Roveri, Biomimetic growth of hydroxyapatite on gelatin films doped with sodium polyacrylate, Biomacromolecules 1 (4) (2000) 752–756.
[16] J.D. Hartgerink, E. Beniash, S.I. Stupp, Self-assembly and mineralization of peptide-amphiphile nanofibers, Science 294 (5547) (2001) 1684–1688.
[17] M. Kikuchi, S. Itoh, S. Ichinose, K. Shinomiya, J. Tanaka, Self-organization mechanism in a bone-like hydroxyapatite/collagen nanocomposite synthesized in vitro and its biological reaction in vivo, Biomaterials 22 (13) (2001) 1705–1711.
[18] Y. Yang, J.L. Magnay, L. Cooling, A.J. El Haj, Development of a 'mechano-active' scaffold for tissue engineering, Biomaterials 23 (10) (2002) 2119–2126.
[19] S.-N. Park, J.-C. Park, H.O. Kim, M.J. Song, H. Suh, Characterization of porous collagen/hyaluronic acid scaffold modified by 1-ethyl-3-(3-dimethylaminopropyl) carbodiimide cross-linking, Biomaterials 23 (4) (2002) 1205–1212.
[20] W. Zhang, S.S. Liao, F.Z. Cui, Hierarchical self-assembly of nano-fibrils in mineralized collagen, Chem. Mater. 15 (16) (2003) 3221–3226.
[21] B. Zhao, H. Hu, S.K. Mandal, R.C. Haddon, A bone mimic based on the self-assembly of hydroxyapatite on chemically functionalized single-walled carbon nanotubes, Chem. Mater. 17 (12) (2005) 3235–3241.
[22] A.B. Descalzo, R. Martínez-Máñez, R. Sancenón, K. Hoffmann, K. Rurack, The supramolecular chemistry of organic-inorganic hybrid materials, Angew. Chem. Int. Ed. 45 (36) (2006) 5924–5948.
[23] H.F. Chen, B.H. Clarkson, K. Sun, J.F. Mansfield, Self-assembly of synthetic hydroxyapatite nanorods into an enamel prism-like structure, J. Colloid. Interface Sci. 288 (1) (2005) 97–103.
[24] S.I. Stupp, P.V. Braun, Molecular manipulation of microstructures: biomaterials, ceramics, and semiconductors, Science 277 (5330) (1997) 1242–1248.
[25] J.D Chen, Y.J. Wang, K. Wei, S.H. Zhang, X.T. Shi, Self-organization of hydroxyapatite nanorods through oriented attachment, Biomaterials 28 (2007) 2275–2280.
[26] F. Ye, H.F. Guo, H.J. Zhang, Biomimetic synthesis hydroxyapatite mediated surfactants, Nanotechnology 19 (2008), 245605 (7 pp).
[27] J.X. Zhang, M. Iwasa, D.L. Jiang, Size-controlled hydroxyapatite nanoparticles as self-organized organic–inorganic composite materials, Adv. Sci. Technol. 53 (2006) 32–37.
[28] E. Landi, A. Tampieri, G. Celotti, S. Sprio, Densification behaviour and mechanisms of synthetic hydroxyapatites, J. Eur. Ceram. Soc. 20 (2000) 2377–2387.
[29] L.M. Rodríguez-Lorenzo, M. Vallet-Regí, Controlled crystallization of calcium phosphate apatites, Chem. Mater. 12 (2000) 2460–2465.
[30] L.C. Palmer, C.J. Newcomb, S.R. Kaltz, E.D. Spoerke, S.I. Stupp, Biomimetic systems for hydroxyapatite mineralization inspired by bone and enamel, Chem. Rev. 108 (11) (2008) 4754–4783.
[31] M. Cao, Y. Wang, C. Guo, Y. Qi, Y. Hu, Preparation of ultrahigh aspect-ratio hydroxyapatite nanofibers in reverse micelles under hydrothermal conditions, Langmuir 20 (2004) 4784–4786.
[32] S. Koutsopoulos, Synthesis and characterization of hydroxyapatite crystals: a review study on the analytical methods, J. Biomed. Mater. Res. 62 (4) (2002) 600–612.
[33] H.N. Patrick, G.G. Warr, Self-assembly structures of nonionic surfactants at graphite–solution interfaces: 2. Effect of polydispersity and alkyl chain branching, Colloids Surf. A: Physicochem. Eng. Aspects 162 (2000) 149–157.
[34] R.J. Robson, E.A. Dennls, The size, shape, and hydration of nonionic surfactant micelles. Triton X-100, J. Phys. Chem. 81 (11) (1977) 1075–1078.
[35] D. Walsh, J.L. Kingston, B.R. Heywood, S. Mann, Influence of monosaccharides and related molecules on the morphology of hydroxyapatite, J. Cryst. Growth 133 (1993) 1–12.
[36] W.J. Cook, C.E. Bugg, Calcium binding to galactose. Crystal structure of a hydrated alpha-galactose–calcium bromide complex, J. Am. Chem. Soc. 95 (19) (1973) 6442–6446.